ELSEVIER

Polymer 40 (1999) 1709–1717

polymer

Time-resolved study of electro-optic property in itaconate copolymer bearing an aminonitrostilbene chromophore

Dong Hoon Choi

Division of Textile, Chemical, and Industrial Engineering, Institute of Material Science and Technology, I.L.R.I, Kyung Hee University, Kyungki 449-701, South Korea

Received 14 April 1998; accepted 21 May 1998

Abstract

The second-order nonlinear optical (NLO) itaconite copolymer was synthesized to study the effect of temperature and time on the electro-optic effect. The aminonitrostilbene chromophore was synthesized to be bound to itaconate polymer backbone. Particularly, two chromophoric groups were present to enhance the dipole moment in one repeating unit of polyitaconate. The resistance and electric potential between the two electrodes were characterized with temperature. The electro-optic signal and coefficient were investigated using the modified reflection technique. The time-resolved study gave much information on how the electro-optic property can be brought about. Temporal stability was also observed at various temperatures, which is around and far below glass transition temperature. © 1999 Elsevier Science Ltd. All rights reserved.

Keywords: Electro-optic; Itaconate copolymer; Pulse poling

1. Introduction

Organic nonlinear optical (NLO) materials provide strong potential advantages for second harmonic generation and electro-optic applications [1–4]. Particularly, side-chain NLO polymers have drawn remarkable interest, in recent years, as promising candidates for application in electro-optic and photonic devices [1–6]. Second-order NLO properties of poled polymers have been extensively studied in the past. Much effort has been made to improve temporal stability of dipolar alignment after poling. Polymers whose glass transition temperatures are very high and crosslinked polymers were adopted for this purpose [7–9]. Although both methods have been proven to be effective in preventing the dipolar relaxation, it should be pointed out that achieving a higher level of molecular alignment, namely a high second-order NLO coefficient, is very difficult or limited with these methods. Meanwhile, poling and its effects have not been seriously considered in the field of polymer physics. Most physical properties in organic polymers are strongly related to the temperature in their environment. Thermodynamically, the polymers exhibited various thermal transition behaviours via molecular relaxation. Therefore, many workers have poled the NLO samples in the vicinity of the glass transition temperature. However, the electro-optic effect can be induced by the change of the transition dipole moments in the matrix, although the extent of change is relatively small. The side chain in the amorphous polymer was covalently bound through a flexible spacer for increase of its mobility at the glass transition temperature (T_g). The side chain group is very long and bulky, and can be divided by a few nodes. Usually the repeated unit of the main chain does not have a permanent dipole moment ($\mu_g = 0$). The second-order NLO effect can be induced by the disruption of centrosymmetry in the side chain group. At T_g, of course, the side chain mobility will be maximized due to the largest segmental motion in the main chain. However, at far below T_g, a smaller scale of 'nodal motion' will be available due to the thermal energy. Then, we can expect the electro-optic (E/O) signal at that low temperature, although it will be relatively small compared to that at T_g. This can be analysed by time-resolved study with the temperature of the matrix [10,11]. Time-resolved techniques permit us to monitor either the relaxation dynamics of the electro-optic signal, following conventional poling of the material, or molecular dynamics during the pulse poling step. In an attempt to both maximize the second-order NLO effect and investigate its temporal stability, we designed and synthesized the itaconate copolymer. Poling conditions were fully optimized to maximize the electro-optic effect of synthesized copolymer.

PII: S0032-3861(98)00405-4

2. Experimental

2.1. Materials and instrumentation

4-Fluorobenzaldehyde, 2-methylaminoethanol, itaconic acid, triphenylphosphine and diisopropyl azodicarboxylate (DIAD) were purchased from Aldrich Chem. Co. and used after purification. Analytical grade reagents and solvents were used without further purification. Commercial grade solvents and reagents were purified using standard techniques. Azobisisobutyronitrile (AIBN) was recrystallized into acetone just before polymerization.

The synthesis of 4-hydroxyethylmethylamino-4′-nitrostilbene (HEANS) and its methacrylate monomer were synthesized following a known procedure [12].

2.1.1. Synthesis of 2-methylene succinic acid bis-(2-{methyl-[4-[2-(4-nitrophenyl)vinyl]-phenyl-amino}ethyl) ester

4-[(6-Hydroxyhexyl)methylamino]-4]-nitrostilbene (HEANS) was reacted with itaconic acid using the Mitsunobu reaction. HEANS (2.98 g, 0.01 mol) was dissolved in 50 ml tetrahydrofuran (THF). Triphenylphosphine (6.55 g, 0.025 mol), dissolved in 10 ml THF, was added. The solution was stirred under purging of argon gas at room temperature. A solution containing 4.04 g (0.02 mol) diisopropyl azodicarboxylate and 0.72 g (0.055 mol) itaconic acid in 10 ml THF was added dropwise over a period of 40 min. The progress of the reaction was checked by thin-layer chromatography (TLC). The reaction was completed in 2 h. The solution was cooled in the freezer and a red solid was filtered. The crude product was recrystallized from acetonitrile to get pure itaconate, m.p. 155.5°C.

^{1}H-nuclear magnetic resonance (n.m.r.) (200 MHz, DMSO-d_6): (ppm) 8.18(d, 4H), 7.79(d, 4H), 7.51(d, 4H), 7.40(d, 2H), 7.10(d, 2H), 6.72(m, 4H), 6.12(s, 1H), 5.72(s, 1H), 4.20(t, 4H), 3.61(t, 4H), 3.22(s, 2H), 2.98(d, 6H).

Anal.: $C_{39}H_{38}N_4O_8$ (690.75), Calcd. C 67.8, H 5.54, N 8.11; Found C 67.5, H 5.61, N 8.09.

2.1.2. Synthesis of copolymer

An equimolar mixture of NLO itaconate and methyl methacrylate (MMA) was dissolved in freshly distilled *N*-methyl pyrrolidinone (NMP) to a total monomer concentration of 0.4 mol l^{-1}. Azobisisobutyronitrile (AIBN, 2 mol% with respect to total monomer) was added to the monomer solution. The solution was taken in vacuum ampoules and freed from dissolved gases by a repeated freeze–thawing technique. The ampoules were placed in an oil bath maintained at 75°C and the solution was kept under stirring for 72 h. The copolymer was precipitated into hot ethanol. The precipitated copolymers were purified by successive reprecipitation from THF into *n*-hexane and ethanol. The pure copolymers were filtered and dried under reduced pressure at 80°C for 48 h; the yield was 28%.

2.1.3. N.m.r. spectroscopy

Proton n.m.r. was recorded with Varian 200 NMR spectrometer. Chloroform-*d* ($CDCl_3$) and DMSO-d_6 were used as solvents for recording n.m.r. spectra. Copolymer compositions were determined by using the n.m.r. peak integration method.

2.1.4. Gel permeation chromatography

The number-average molecular weight (M_n) and molecular weight distribution were determined by employing Waters gel permeation chromatograph (Model 440) attached with a 410 diffraction refractometer. Spectral grade THF was used as solvent and molecular weight calibration was done using polystyrene standard.

2.1.5. Material processing for electro-optic study

The copolymers were dissolved in 1,1,2,2-tetrachloroethane. For studying the NLO effect, thin films were fabricated on indium tin oxide (ITO) precoated glass by using a filtered solution. The refractive index (n) and thickness of the film coated on silicon wafer were measured with a Metricon instrument simultaneously at three different wavelengths (632, 1300 and 1550 nm). For linear electro-optic coefficient measurement, we deposited the gold electrode on top of the film to fabricate sandwiched samples.

2.1.6. In-situ pole and probe method of electro-optic effect

We measured the linear electro-optic coefficient, r_{33}, of the samples by way of reflection technique, which is based on the difference of phase retardation in transverse electric (TE) and transverse magnetic (TM) mode [13,14]. Wavelengths of 632, 830, and 1300 nm were used for this measurement. The sine wave voltage (10 V_{rms} at 1 kHz) was applied to each sample during recording of the modulated signal. The linear electro-optic coefficient, r_{33} of the new copolymer film was calculated by the following equation.

$$r_{33} = \frac{3\lambda I_m}{4\pi V_m I_c n^2} \frac{(n^2 - \sin^2\theta)\frac{1}{2}}{\sin^2\theta} \quad (1)$$

Where I_m is the amplitude of electro-optic modulation, V_m is the a.c. voltage applied to the sample, and I_c is the intensity of incident light where phase retardation is 90° between the TE and TM modes.

For time-resolved E/O study, the sample was placed on the heater to apply d.c. and a.c. voltage by using a computer controlled switching device. Poling was performed for any time period and the E/O modulated signal was integrated during the period when a.c. voltage was being applied (See Fig. 1) [10,11].

2.1.7. Measurement of relative resistance of the thin film with temperature

The resistance of the polymer film used could not be measured using a digital multimeter because the resistance is usually out of the limit of the measuring range. We

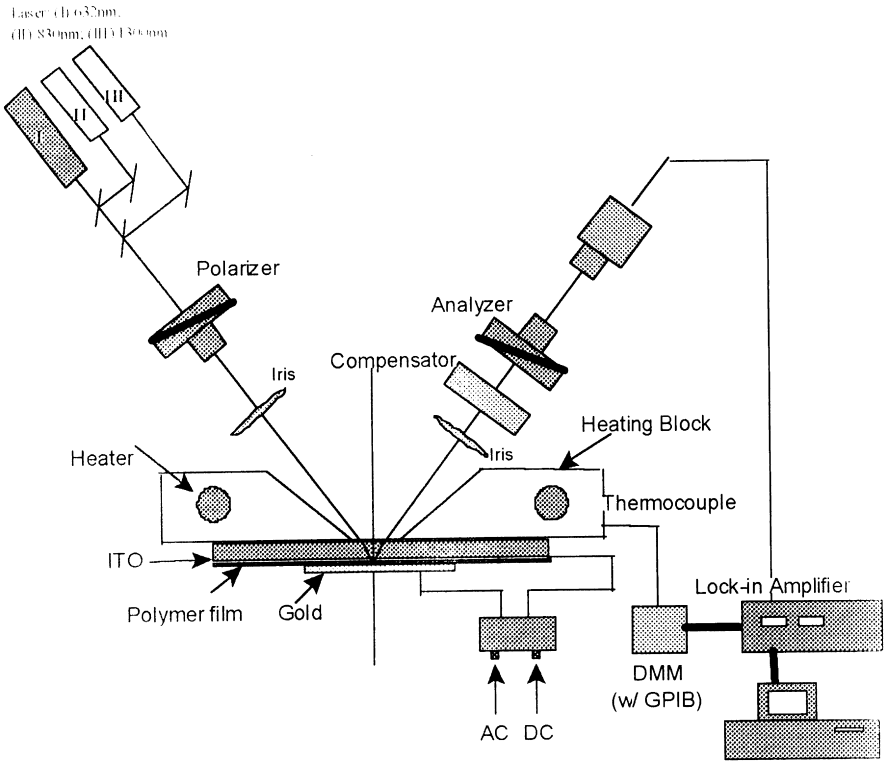

Fig. 1. In situ electro-optic signal measurement setup.

connected a ~50 MΩ (50, 628, 288 Ω) resistor to film in a parallel way to monitor the change of the overall resistance. The film was mounted on the precision controlled heater. With the increase of the temperature, two digital multimeters (Keithley 2000, Fluke 45D) measured the overall resistance and the temperature of the sample instantaneously.

2.1.8. Measurement of electric potential between the two electrodes during poling

We investigated the change of the electric potential when the d.c. electric field was applied during poling. Additionally, we could observe the dielectric breakdown voltage as the temperature of the sample was changed. The feature of the sample is identical to that for the electro-optic study. In order to monitor the applied voltage between the gold and ITO electrode, we connected ~1 MΩ (937 544 Ω) resistor in a serial manner. The film was mounted on the heater to increase the temperature of the sample. The sample started to be heated applying the electric poling field. In this experiment, 20–50 V d.c. was applied to this circuit. We monitored the potentials both in the film and in the resistor at the same time. The sum of the potentials is identical to the applied voltage. The temperature and two electric potentials were integrated with the uniform time interval.

3. Results and discussion

The present work describes the preparation of second-order nonlinear optical active polymers with novel structure and chromophore for attaining the high NLO activity for practical use. Additionally, we postulated how the poling efficiency can be maximized by optimal poling conditions. The method for poling suggested in the past was modified fully by the other serial techniques without T_g from differential scanning calorimetry (d.s.c.).

Fourier transform infra-red (*FT*i.r.) and nuclear magnetic resonance (*FT*n.m.r.) spectroscopy determined the structure of synthesized compound and the molar composition of monomer in the copolymer. The synthetic procedure and the structure of the copolymer are shown in Fig. 2. The copolymers are red in colour and well soluble in THF, cyclohexanone, dimethyl formamide, dioxane, etc. although the solubility of itaconate monomer is relatively poor.

3.1. Composition and molecular weight

The comonomer feed ratio was maintained at 1/1 (mol/mol) in this case. The resultant mole ratio of copolymer is found to be 1/0.36 (MMA/NLO itaconate). The proportion of NLO unit in the copolymer is quite low. This may be due to the lower reactivity ratio of the itaconate monomer and the effect of retardation in the polymerization rate from the terminal nitro group in the NLO monomer. The molecular

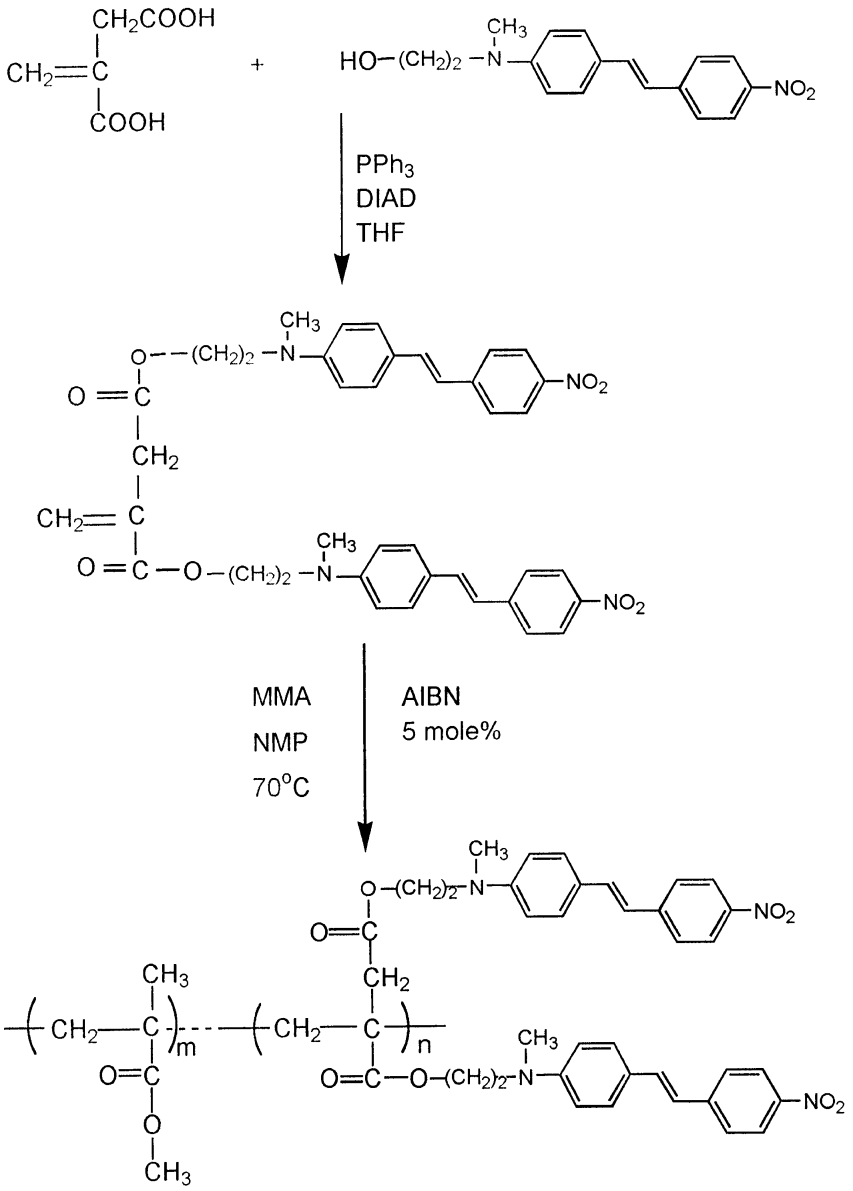

Fig. 2. Synthetic procedure and the structure of itaconate copolymer bearing the NLO chromophore.

weight (M_n) and polydispersity of the copolymers are 32 700 and 2.15 respectively. Resulting from the molecular weight, the film-forming property was expected to be well defined after spin-coating.

3.2. Electrical properties of the copolymer with temperature

We investigated the relative resistance of the polymer films with change of temperature. In general, the metal showed an increase of the resistance as the temperature increased. However, in semiconductor and organic polymers the resistance would be lessened with temperature. In the new copolymer, the resistance started to decrease from 115°C, and then abruptly decreased around 130°C in the heating cycle. We cooled the sample while measuring the resistance. In the cooling cycle the resistance was fully recovered. The temperature at which the resistance reached the maximum was shifted to a slightly higher one, around 120°C. Therefore, we could observe a 'transition temperature' at which the resistance was largely changed. Although the absolute value of the resistivity of the copolymer film was not calculated, and also the dielectric behaviour was not taken into account, we could roughly observe the reversible behaviour of resistance of the medium with temperature (see Fig. 3).

In addition to the previous experiment, we tried to measure the potential that can be applied to the polymer film itself during poling. We connected the low ohmic resistor (~1 MΩ) to the film in a serial manner. The polymer film was placed on the heater whose temperature was recorded by a digital multimeter with a K-type thermocouple. Resulting from the previous experiment, the

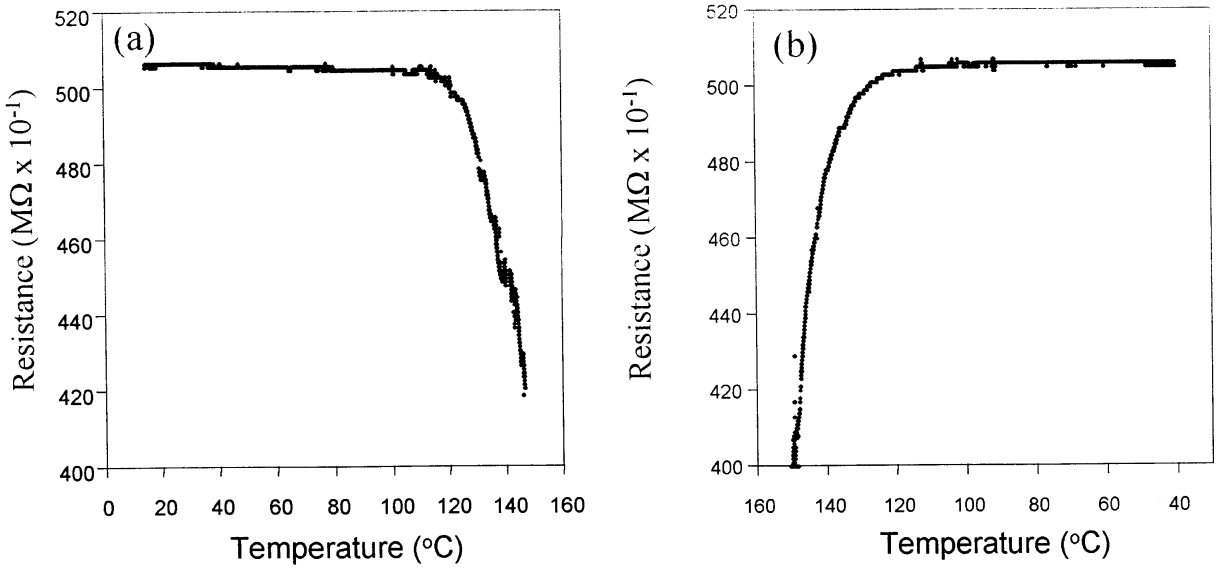

Fig. 3. Temperature dependence of relative resistance: (a) heating cycle; (b) cooling cycle.

resistance of the medium was varied with the temperature. We applied 27 V to the two electrodes from a d.c. power supplier. The voltage we applied was mostly monitored from the sample unit, initially at room temperature. When the temperature of the sample was raised to 120°C, the potential to the sample decreased slowly, and finally at 138°C the voltage to the sample was almost zero, due to the dielectric breakdown. Most of the applied voltage was monitored on the low ohmic resistor. This indicates that the samples were broken down dielectrically. In Fig. 4, we could observe the onset temperature at which the potential is abruptly decreased. The onset temperature is around 123°C, which is very close to the transition temperature at which the resistance dropped sharply during heating. This indicates that the applied voltage can be loaded mostly to the sample, although the resistance decreased slightly. From this experiment, we could observe the dielectric breakdown temperature, even though the temperature is dependent on the applied voltage. When applying 40, 60 and 80 V to the sample, the breakdown temperature was observed ranging

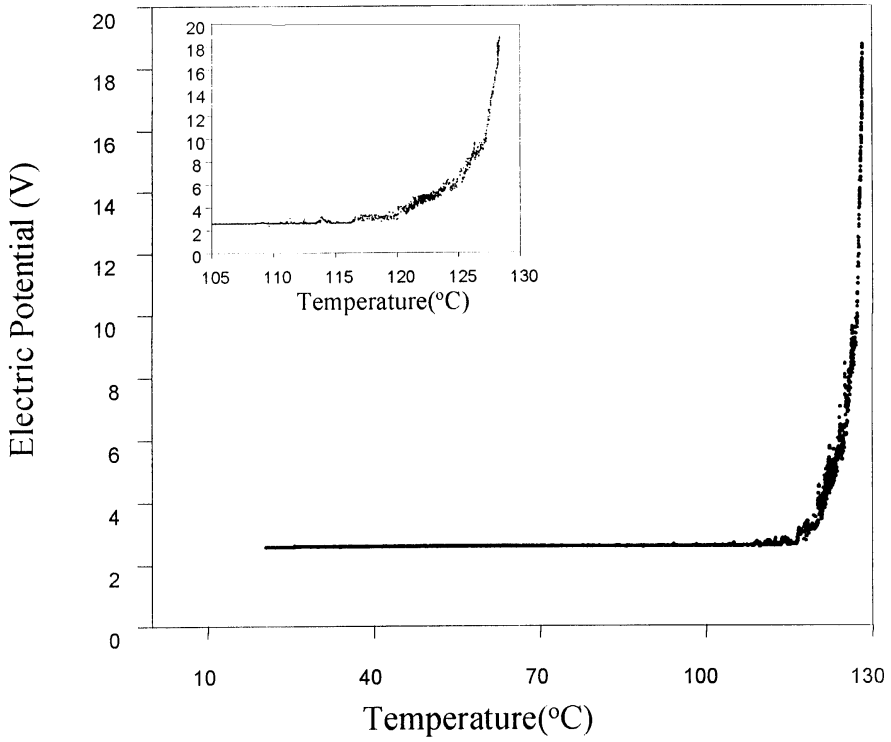

Fig. 4. Temperature dependence of electric potential on 1 MΩ resistor that is connected to the sample in a serial way.

from 130 to 140°C. Therefore, during poling, we cannot induce the noncentrosymmetry, i.e. alignment of polar molecules in the side chain at a temperature higher than this breakdown temperature. The poling temperature of the copolymer films was tentatively determined to be around 118–120°C.

3.3. Time resolved study of electro-optic properties using pulse poling technique

Resulting from the above series of experiments, we could see the optimal poling temperature and poling field. In this section, we will show the electro-optic properties of the polymer under various conditions. Firstly, we poled the copolymer film under 100 V mm^{-1} at an optimal temperature (118°C) for 10 min, following the normal electrode poling technique. The refractive indices were measured by Metricon at three different wavelengths (632, 1300, 1500 nm). The data was fitted to the Sellmeir equation to obtain the theoretical indices at TE and TM mode in the case of the index at 830 nm. Before poling, the index at TM mode (1.728) is slightly higher than that at TE mode (1.692), at 632.8 nm. Electro-optic coefficients, r_{33}, were determined as 245.0, 56.9 and 24.6 pm V^{-1} at 632.8, 830 and 1300 nm, respectively. These values are relatively higher than that obtained from a methacrylate–MMA copolymer bearing the same chromophore. As we expected, this copolymer showed quite high electro-optic coefficients at three different wavelengths, because the poling condition was optimally maximized.

In Fig. 5, we measured the electro-optic signal and calculated the r_{33} with the change of poling voltage at three different wavelengths. The r_{33} values are observed to be directly proportional to the poling voltage(V_p). Even under 100 V μm^{-1}, any saturation of E/O coefficient was not observed.

To measure the electro-optic modulation signal during poling, the reflection technique, proposed earlier, has been widely used by many researchers. Although there are some problems due to the multiple reflection between each boundary, the contribution of induced piezoelectric and electrostrictive effect and imposition of a third-order NLO effect, the linear electro-optic coefficient was measured much more simply and easily than using prism-coupling methods. Recently this setup was modified for investigating the molecular dynamics during poling, and the molecular relaxation behaviour could be observed in-situ after applying both d.c. voltage for poling and a.c. field for integration of the E/O signal. In Fig. 1, the schematic diagram of in-situ measurement setup is illustrated. We can switch between a poling voltage, V_p, and an alternate voltage of amplitude V_m in a periodic way, and study the time and temperature dependence of the r_{33} (t,T). Using the computerized switching device of applying voltage, any selection of poling (t_1) and probing (t_2) times can be adjusted (3 s $< t_1, t_2 <$ infinity).

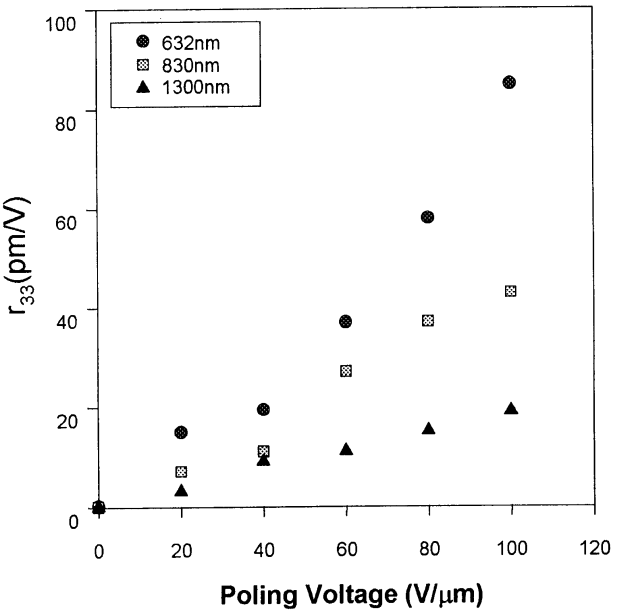

Fig. 5. Poling field dependence of the electro-optic coefficients at 632.8, 830 and 1300 nm wavelengths.

In this study, we placed the sample on the heater during heating and cooling cycle. We applied 50 V μm^{-1} to the sample at room temperature. The temperature was programmed to increase at a rate of 10°C min^{-1} and to decrease by approximately 15°C min^{-1}.

We set t_1 and t_2 to be identical at 7.5 s. For every 7.5 s, we poled and integrated the E/O signal of the sample at an instant temperature. As shown in Fig. 6, the temperature dependence of E/O signal appeared. The E/O signal started to increase from 90 to 95°C, that is far below T_g. As the temperature increased, the signal also increased gradually. As the temperature is higher than 120°C, the E/O signal decreased gradually. In Fig. 7, the temperature started to decrease from 144°C to room temperature, in the presence of pulse-applied voltages. The lowered E/O signal was recovered again as the temperature decreased. Thereafter, the E/O signal was saturated at a temperature around 120–125°C. From these results, we could know that poling was not effectively performed higher than 125°C. As we observed in the previous electrical measurements, the resistance decreased as the temperature rose. The electric potential drop in the sample happened during heating to pole, and therefore poling temperature is a very important factor to raise the poling efficiency and the value of the E/O modulated signal. The electrical conductivity is strongly increased under high temperature and high electric field. After the first cooling cycle, the resistance of the film was recovered and the pulsed d.c. field can lead to a raising of the E/O signal again. The signal value was maintained until cooling to room temperature in the presence of a pulsed field. Another phenomenon was that E/O signal was observed even at well below T_g. As we can see in Fig. 6, the signal started to increase at 90–95°C. This temperature is 24–19°C below the T_g that was

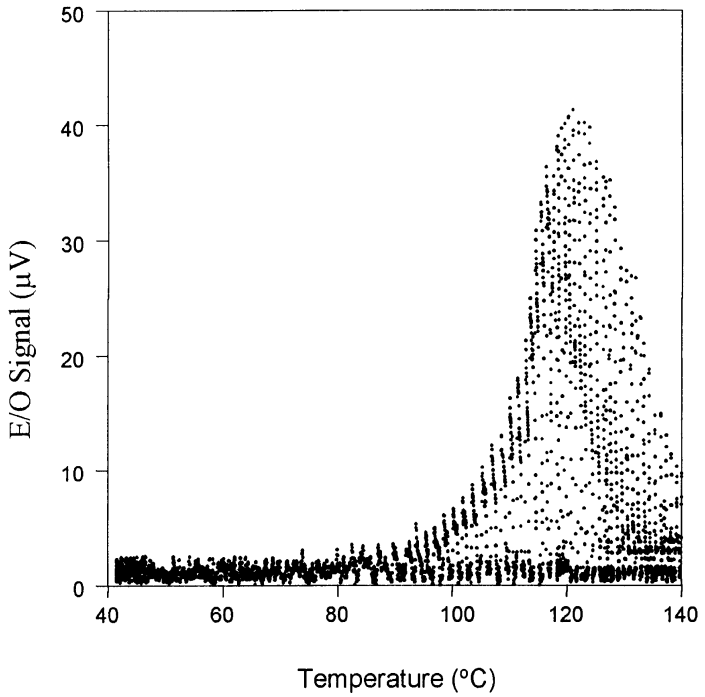

Fig. 6. Change of the E/O signal during heating under pulsed poling.

determined from d.s.c. thermal analysis. This indicates that the origin of the E/O effect can be attributable to the segmental motion in the polar molecule. The motion of the polar molecule will be, of course, much enhanced in the vicinity of T_g. However, the small segmental motion at some nodes can cause a change of the transition dipole moments ($\Delta\mu = \mu_e - \mu_g$), because there is a flexible bond in the side chain of this polymer. The origin of the E/O effect can be considered from the polar side group itself. Once the environmental conditions give some degree of freedom to the polar molecules, the applied field can generate the change of the dipole moment during poling. This can provide some extent of electron delocalization to induce the enhancement of dipole moment.

In Fig. 8, we could observe the decaying behaviour of the E/O signal at different temperatures. We set the poling time and probing time to be 50 and 150 s respectively under 50 V μm^{-1}. We changed the sample temperature to 116°C

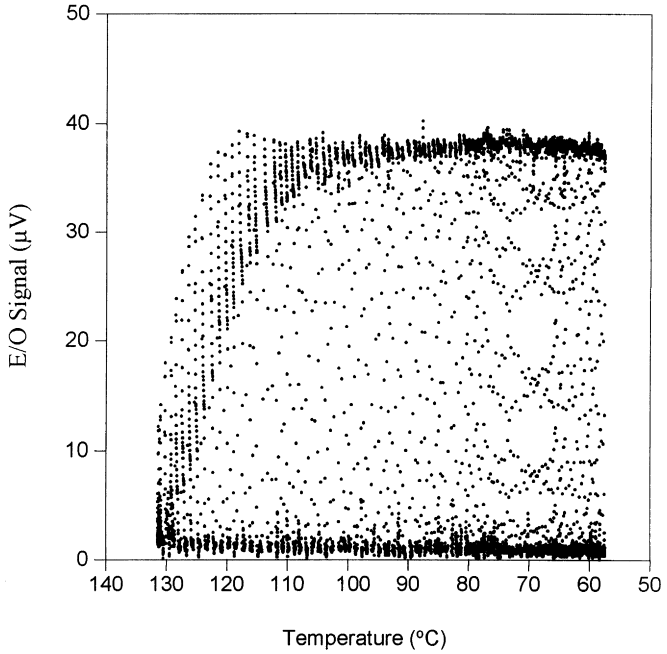

Fig. 7. Change of the E/O signal during cooling under pulsed poling.

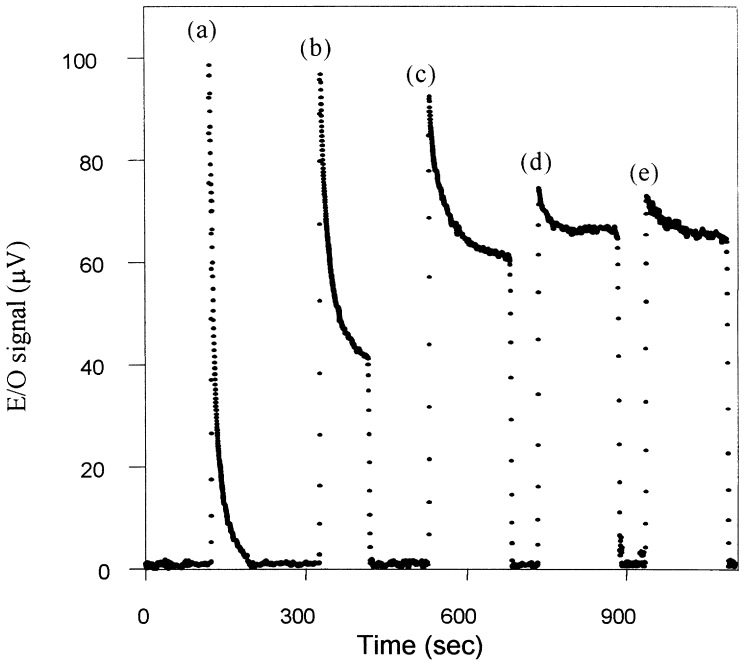

Fig. 8. Decaying behaviour of the E/O signal at different temperatures: (a) 116°C; (b) 106°C; (c) 96°C; (d) 78°C; (e) 68°C.

(a), 106°C (b), 96°C (c), 78°C (d), and 68°C (e), to trace the decay of the E/O signal. At each temperature, the relaxation behaviours were clearly defined. The relaxation time, τ, and average relaxation time constant $\langle\tau\rangle$, can be obtained by using the Kohlrausch–Williams–Watts (KWW) stretched exponential function. That is strongly dependent on the temperature of the sample. The analysis results are shown in Table 1. We employed the average relaxation time constant, $\langle\tau\rangle$ represented as follows:

$$\langle\tau\rangle = (\tau/\beta)\Gamma(1/\beta) \quad (2)$$

As we expected, the relaxation time, τ, decreases with increasing temperature, T, from about 26 h at 68°C below $T_g = 114$°C to about 8.608 s at $T = 116$°C.

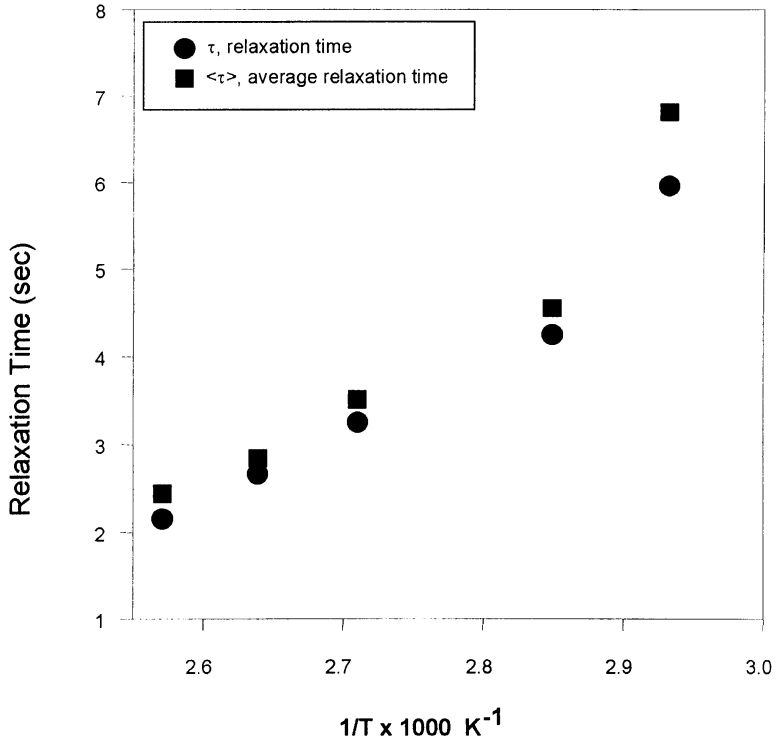

Fig. 9. Relationship between the relaxation time, τ, and $1/T$ (absolute temperature) at which the decaying behaviour of E/O signal was observed.

Table 1
Parameters obtained from curve fitting the experimental decaying curve at each temperature to stretched exponential function and average relaxation times

Temperature (°C)	τ (s)	$\langle\tau\rangle$ (s)	β_ω
116.0	8.608	11.485	0.664
106.0	14.315	17.119	0.747
96.0	25.690	33.215	0.685
78.0	69.795	94.6277	0.653
68.0	387.236	911.2494	0.461

$I(t) = I_0 \exp(-(t/\tau)^{\beta_\omega}) + R$ [11]

In Fig. 9, the temperature dependence of τ is shown from the data of Table 1. The curve shows an Arrhenius temperature dependence for $T < T_g$. The curve is fitted to Arrhenius behaviour with an activation energy of $E_a = 14.97$ kcal mol^{-1}, which is smaller than that of a usual guest–host NLO polymer system (5 kcal mol^{-1}, measured and calculated value using 10 wt% Disperse red 1 in PMMA), indicating the better stability of the E/O effect after measuring in an identical way.

In conclusion, the results allow us to choose the possibility of pulse-poling, that can be operated to obtain an effective poling of the polymer films. Under the investigation of the temperature dependence of relative resistance in a stationary state and the change of electric potential between the electrodes during poling, the poling efficiency can be optimized and the electro-optic coefficient, r_{33} can be maximized compared to the value obtained by others. In the material respect, the itaconate copolymer showed a higher electro-optic effect than the methacrylate copolymer loaded with the same amount of chromophore, because the steric hindrance between NLO itaconate and MMA was much released. The molecular alignment of the polar side chain can become larger than that of the other copolymer whose repeating unit contains one chromophore itself. The order parameter, A_2, obtained by polarized absorption spectroscopy was determined to be around $0.23 \sim 0.24$, much higher than the reported value [15].

Acknowledgements

This research was supported by Korea Science and Engineering Foundation (Haeksim Research 1998).

References

[1] Prasad PN, Williams DJ, editors. Introduction to nonlinear optical effects in molecules and polymers. New York: Wiley, 1991.
[2] Prasad PN, Ulrich DR, editor. Nonlinear optical and electroactive polymers. New York: Plenum Press, 1988.
[3] Hann RA, Bloor D, editors. Organic molecules for nonlinear optics. London: The Royal Society of Chemistry, 1989.
[4] Messier J, Kajzar F, Prasad PN, Ulrich DR, editors. Nonlinear optical effects in organic polymers. Dordrecht: Kluwer Academic Publishers, 1989.
[5] Ahlheim M, Barzoukas M, Bedworth PV, Blanchard-Desce M, Fort A, Hu Z-Y, Marder SR, Ferry JW, Runser C, Staehelin M, Zysset XX Science 1996;271:335.
[6] Burland DM, Miller RD, Walsh CA. Chem Rev 1994;94:31.
[7] Nemoto N, Miyata F, Nagase Y, Abe J, Hasegawa M, Shirai Y. Chem Mater 1997;9:304.
[8] Saadeh H, Gharavi A, Yu D, Yu L. Macromolecules 1997;30:5403.
[9] Wang X, Kumar J, Triphathy SK, Li L, Cheng JI, Marturunkkakul S. Macromolecules 1997;30:219.
[10] Michelotti F, Toussaere E, Levenson R, Liang J, Zyss J. Appl Phys Lett 1995;67:2765.
[11] Michelotti F, Toussaere E, Levenson R, Liang J, Zyss J. J Appl Phys 1996;80 (3):1773.
[12] Demartino RN. (Hoecht Celanese Corp.), European Patent No. 0294706, 1988.
[13] Shuto Y, Amano M. J Appl Phys 1995;77 (9):91.
[14] Teng CC, Man HT. Appl Phys Lett 1990;56 (18):1734.
[15] Graf HM, Zobel O, East AJ, Haarer D. J Appl Phys 1994;75 (7):3335.